

FIRST DEMONSTRATION OF ELECTRON BEAM GENERATION AND CHARACTERIZATION WITH AN ALL SUPERCONDUCTING RADIO-FREQUENCY (SRF) PHOTOINJECTOR*

T. Kamps[#], W. Anders, R. Barday, A. Jankowiak, J. Knobloch, O. Kugeler,
 A. Matveenko, A. Neumann, T. Quast, J. Rudolph, S. Schubert, J. Völker
 Helmholtz-Zentrum Berlin, Berlin, Germany
 P. Kneisel, JLAB, Newport News, Virginia, USA
 R. Nietubyc, A. Soltan Institute, Swierk/Otwock, Poland
 J. Sekutowicz, DESY, Hamburg, Germany
 J. Smedley, BNL, Upton, New York, USA
 V. Volkov, BINP, Novosibirsk, Russia
 G. Weinberg, FHI/MPG, Berlin, Germany
 I. Will, Max-Born-Institute, Berlin, Germany

Abstract

In preparation for a high brightness, high average current electron source for the energy recovery linac BERLinPro an all superconducting radio-frequency (SRF) photoinjector is now in operation at Helmholtz-Zentrum Berlin. The aim of this experiment is beam demonstration with a high brightness electron source able to generate short, few ps long pulse length electron bunches from a superconducting (SC) cathode film made of Pb coated on the backplane of a Nb SRF cavity. This paper describes the setup of the experiment, first results from beam measurements and capabilities of the source derived from beam dynamics considerations.

In April 2011 the photoinjector generated and accelerated for the first time electron beam. This result marks the highlight of the project running for two years starting with project approval in May 2009.

MOTIVATION

Modern accelerator based light sources like Energy Recovery Linac (ERL) driven synchrotron radiation sources, Free Electron Lasers (FEL), or THz radiation sources require injectors capable of delivering high-brightness electron beams at high average current with near-continuous operation.

HZB will explore the ERL paradigm as a driver accelerator for next generation light sources with the ERL test facility BERLinPro [1], a fully integrated test accelerator with all components and infrastructure required to build a full-scale ERL. The baseline design of BERLinPro calls for an SRF photoinjector able to deliver an average current of 100 mA with bunches with low emittance of better than 1 mm mrad which can be compressed to ps-level bunch length [2].

The choice of photocathode material is of paramount importance for the SRF photoinjector. The initial electron beam parameters, like thermal emittance, pulse length,

and average current are determined by the photocathode and drive laser properties. The SRF environment of the accelerating cavity places additional considerations. Any normal conducting cathode material needs to be electrically insulated against the SC cavity material. The RF choke filter by Volkov [3] is an attractive solution for this and enables the use of nearly all available photocathode materials like multi-alkali (CsK₂Sb) or other semiconductor compounds with quantum efficiencies in the region of 10⁻¹ to 10⁻² for visible wavelengths.

FELs and THz radiation applications ask for high transverse peak brightness and only moderate average currents in the order of 1 mA. The requirements on the photocathode are more relaxed concerning high average current, which would allow the use of metallic photocathodes with all its benefits and drawbacks. The main drawback is the low quantum efficiency of the order of 10⁻³ to 10⁻⁵ for UV wavelengths, the main advantages the long lifetime and ultra-fast response time. Sekutowicz et al developed the idea of the hybrid Nb/Pb gun cavity [4], where a small spot of Pb is deposited on the backplane of the Nb cavity. Several test cavities have been built and all cavity handling procedures have been optimized not to compromise the cavity quality factor Q_0 and achievable gradient with a Pb film present on the backplane [5].

The work presented in this paper takes this idea to a beam experiment. The goal is to build a SRF injector with a hybrid Nb/Pb cavity, characterize the SRF cavity, characterize and laser clean the Pb cathode, and finally generate an electron beam with this setup.

INJECTOR SETUP

The SRF photoinjector was setup in the time from May 2009 to April 2011 at HZB. The experiment makes heavy use of existing SRF infrastructure of the Horizontal Bi-

*Work supported by Bundesministerium für Bildung und Forschung und Land Berlin. The work on the Pb cathode film is supported by EuCARD Grant Agreement No. 227579.

[#]kamps@helmholtz-berlin.de

Cavity Test (HoBiCaT) facility [6]. For the beam experiment with the SRF photoinjector the cryomodule of HoBiCaT had to be modified to get a beam pipe exit. In addition a photocathode drive laser system and a beamline for electron beam diagnostics were installed and setup.

Cold mass – Cavity, Cathode and Solenoid

The microwave design of the SRF cavity (called gun cavity 0.1) is a 1.6 cell 1.3 GHz structure with TESLA-like cups. Gun cavity 0.1 was built, tested, cleaned and assembled at JLAB [7]. During the tests at JLAB, the cavity showed excellent performance, Q_0 exceeding 10^{10} and gradients > 35 MV/m have been measured without Pb film. With the Pb film, Q_0 values in the mid 10^9 region and gradients up to 25 MV/m, limited by field emission, could be achieved.

The Pb cathode film was deposited at A. Soltan Institute with a plasma arc-deposition system, which allows coating of a cavity dressed with its LHe tank [8]. Several witness samples on Nb and Mo substrates have also been deposited at A. Soltan to study the surface morphology and chemistry.

A SC solenoid needs to be placed close to the cavity to focus the diverging beam coming from the cavity. The presence of an additional magnetic field on the cavity surface may lead to severe Q degradation and eventually to a quench, as observed during test measurements with a multi-cell SRF cavity [9]. We decided therefore to place the solenoid in front of the cavity (0.47m from the cathode), and wrap the solenoid and the cavity with mu-metal shield. Fig. 1 shows the complete cold mass of the SRF photoinjector.

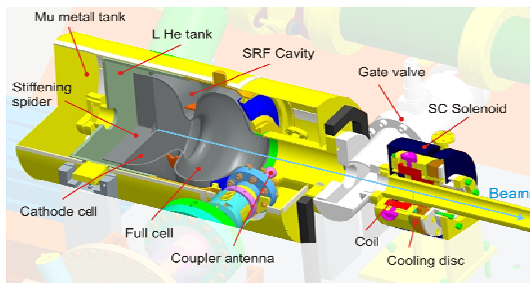


Figure 1: Cold mass of the SRF photoinjector..

Drive laser and electron diagnostics

The photocathode drive laser was developed by MBI and consists of a diode-pumped Yb:YAG oscillator with a diode-pumped regenerative amplifier. The IR output of the amplifier is converted into the UV to $\lambda = 258$ nm by a two stage harmonic generator. The laser pulse length is $\Delta t = 2...3$ ps (fwhm) with pulse energies up to 0.15 μ J. The laser is usually operated at 8 kHz repetition rate.

The electron beam diagnostics beamline allows the measurement of all projected beam parameters [10]. The transverse beam profile can be measured with crystal Ce:YAG viewscreens. The beam current is measured with a retractable Faraday Cup and the beam momentum is

measured with a dipole spectrometer with a viewscreen in the dispersive arm.

LASER CLEANING

Laser cleaning is required to control the state of the cathode surface. During and in between cavity preparation steps, contaminants have been absorbed on the Pb surface, which increase the workfunction of the cathode and thus lowering the QE.

Laser cleaning of the Pb cathode film with a high power excimer laser as suggested by Smedley [11] was central to our investigations. We performed laser cleaning at the injector with both cavity and Pb cathode film in the superconducting state and observed QE, QE map, dark current and other beam parameters before and after laser cleaning [12]. In order to discover the mechanism for QE enhancement we also performed laser cleaning on witness samples at a XPS/ARPES beamline at the synchrotron radiation source Bessy II [13].

PRE-BEAM RESULTS

After installation and cooldown of the cold mass, Q_0 measurements were performed frequently before and after laser cleaning. At HoBiCaT the measured Q_0 was at $4 \cdot 10^9$ with field emission starting at 12 MV/m. The performance could partially recovered during laser cleaning, especially the reduction of unwanted beam production. The cavity was run routinely at field gradients from 12 to 22 MV/m.

Occasionally, cavity field trips can be observed while running the cavity at high gradients and with the drive laser spot on specific points on the Pb cathode. It is possible to process such field trip areas by slowly increasing the power of the drive laser beam [14].

The energy spectrum of the dark current electrons suggests emission in several degL long intervals around 90 degL launch phase with the emission sites located on the backplane close to the cathode. After laser cleaning the onset for field emission moved from 12 to 15 MV/m, suggesting localized levelling of field emitters.

BEAM MEASUREMENTS

In Fig. 2 the beam kinetic energy is shown as a function of injection phase at gradients of 12 and 20 MV/m.

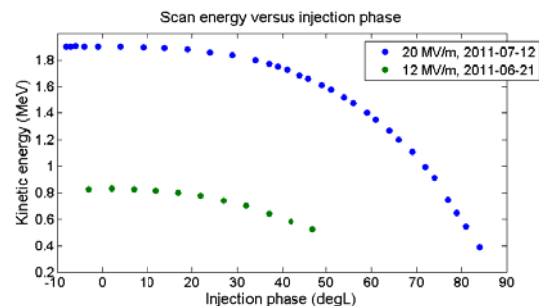


Figure 2: Phase scans of beam kinetic energy for gradients of 12 and 20 MV/m.

The maximum kinetic energy is 1.9 MeV and is reached at 5 degL. Fig. 3 shows a plot of phase scans looking at the extracted charge at two spots on the photocathode with different QEs. The phase window for extraction is roughly 10 degL larger at the high QE location. The curve shape around 0 degL injection phase is proportional to the integral of the bunch length distribution. We see from the plots that the bunch length during extraction is longer for the region QE_{high} compared to the QE_{low} spot, most likely due to the higher charge density at QE_{high} .

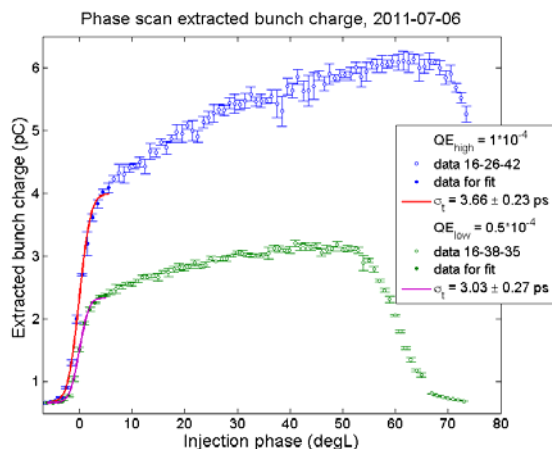


Figure 3: Phase scans at two cathode spots with a gradient of 20 MV/m.

We measured the transverse beam emittance with the solenoid scan technique. Here the procedure consists of a variation of the focal length of the SC solenoid while observing the transverse size of the charge distribution with the first viewscreen. From a plot with the squared beam size versus the solenoid strength we can determine the Twiss parameters of the charge distribution at the entrance of the solenoid by fitting a linear beam optics model to the data.

Fig. 4 shows data and the linear beam optics model for a measurement at 2.5 pC and the injector set to a gradient of 20 MV/m. The foci for the horizontal and vertical plane are shifted indicating astigmatism of the solenoid lens. Furthermore the focused spot size in the horizontal plane is larger compared to the vertical plane, also caused by field errors of the solenoid lens. We found the solenoid also steering in the horizontal direction. From these observations we may conclude that the solenoid has a yaw error leading to astigmatism and higher order contributions to the beam emittance.

We measured the emittance as a function of bunch charge q for 2.5, 1.875 and 1.5 pC and investigated the scaling of the emittance proportional to $q^{2/3}$ [15]. Assuming that the vertical data is following the linear beam optics model and represents the true transverse emittance we can extrapolate a zero charge emittance which should give us already a good indication of the thermal emittance of the cathode.

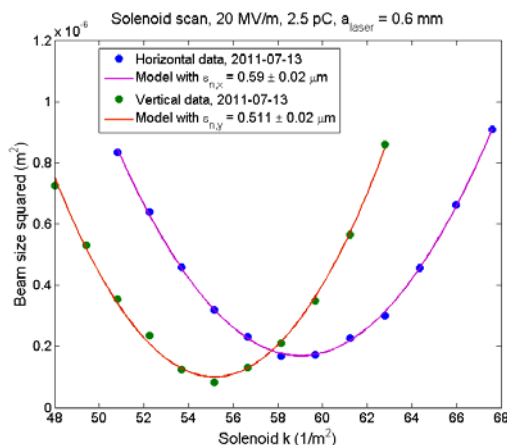


Figure 4: Solenoid scan data and linear beam optics model. The errorbars for the beam size measurement is comparable to the dot size.

For the vertical data only we get a zero charge emittance to laser spot ratio for the Pb cathode of $\epsilon_{zc} = (1.27 \pm 0.39) \mu\text{m}/\text{mm}$ (rms).

CONCLUSIONS & OUTLOOK

First beam with the SRF photoinjector was achieved in April 2011, two years after project approval. Since then, we are following an intense commissioning programme.

For the next run of the SRF photoinjector in the first half of 2012 we plan to install a new gun cavity with tuner system, equip the solenoid with actuators, update the viewscreen system of the diagnostics beamline and improve the Pb cathode deposition and handling systems.

ACKNOWLEDGEMENTS

We thank all colleagues at A. Soltan, BINP, BNL, DESY, FHI/MPG, HZB, JLAB, and MBI for their support in the realization of this project.

REFERENCES

- [1] A. Jankowiak et al, Proc. of LINAC 2010
- [2] T. Kamps et al, J. Phys.:Conf. Ser. 298 012009(2011)
- [3] D. Janssen et al, NIM A 507 (2003) 314
- [4] J. Sekutowicz et al, PRST-AB 8, 010701 (2005)
- [5] J. Sekutowicz et al, Proc. of PAC 2007
- [6] O. Kugeler et al, RSI 81, 074701 (2010)
- [7] P. Kneissel et al, Proc. of PAC 2011
- [8] R. Nietubyc et al, Proc. of LINAC 2010
- [9] O. Kugeler et al, Proc. of SRF 2009
- [10] J. Smedley et al, PRST-AB 11, 013502 (2008)
- [11] R. Barday et al, Proc. of DIPAC 2011
- [12] R. Barday et al, in preparation
- [13] S. Schubert et al, in preparation
- [14] A. Neumann, these proceedings
- [15] J. Rosenzweig, E. Colby, TESLA-Report 1995-04